Scheme for efficient extraction of low-frequency signal beyond the quantum limit by frequency-shift detection

R. G. Yang,[1,2,*] J. Zhang,[1,2] Z. H. Zhai,[1,2] S. Q. Zhai,[1] K. Liu,[1,3] and J. R. Gao[1,2,3]

[1]*State Key Laboratory of Quantum Optics and Quantum Optics Devices, Shanxi University, Taiyuan, 030006, China*
[2]*College of Physics and Electronics Engineering, Shanxi University, Taiyuan, 030006, China*
[3]*Institute of Opto-Electronics, Shanxi University, Taiyuan 030006, China*
**yrg@sxu.edu.cn*

Abstract: Low-frequency (Hz~kHz) squeezing is very important in many schemes of quantum precision measurement. But it is more difficult than that at megahertz-frequency because of the introduction of laser low-frequency technical noise. In this paper, we propose a scheme to obtain a low-frequency signal beyond the quantum limit from the frequency comb in a non-degenerate frequency and degenerate polarization optical parametric amplifier (NOPA) operating below threshold with type I phase matching by frequency-shift detection. Low-frequency squeezing immune to laser technical noise is obtained by a detection system with a local beam of two-frequency intense laser. Furthermore, the low-frequency squeezing can be used for phase measurement in Mach-Zehnder interferometer, and the signal-to-noise ratio (SNR) can be enhanced greatly.

OCIS codes: (270.0270) Quantum optics; (270.6570) Squeezed states; (120.3180) Interferometry.

References and links

1. K. McKenzie, N. Grosse, W. P. Bowen, S. E. Whitcomb, M. B. Gray, D. E. McClelland, and P. K. Lam, "Squeezing in the audio gravitational-wave detection band," Phys. Rev. Lett. **93**(16), 161105 (2004).
2. H. Vahlbruch, S. Chelkowski, B. Hage, A. Franzen, K. Danzmann, and R. Schnabel, "Demonstration of a squeezed-light-enhanced power- and signal-recycled Michelson interferometer," Phys. Rev. Lett. **95**(21), 211102 (2005).
3. G. Q. He, S. W. Zhu, H. B. Guo, and G. H. Zeng, "Security of quantum key distribution using two-mode squeezed states against optimal beam splitter attack," Chin. Phys. B **17**(4), 1263–1268 (2008).
4. A. Furusawa, J. L. Sorensen, S. L. Braunstein, C. A. Fuchs, H. J. Kimble, and E. S. Polzik, "Unconditional quantum teleportation," Science **282**(5389), 706–709 (1998).
5. A. M. Lance, T. Symul, W. P. Bowen, B. C. Sanders, and P. K. Lam, "Tripartite quantum state sharing," Phys. Rev. Lett. **92**(17), 177903 (2004).
6. V. Josse, M. Sabuncu, N. J. Cerf, G. Leuchs, and U. L. Andersen, "Universal optical amplification without nonlinearity," Phys. Rev. Lett. **96**(16), 163602 (2006).
7. J. Jing, J. Zhang, Y. Yan, F. Zhao, C. Xie, and K. Peng, "Experimental demonstration of tripartite entanglement and controlled dense coding for continuous variables," Phys. Rev. Lett. **90**(16), 167903 (2003).
8. S. L. Braunstein and P. V. Loock, "Quantum information with continuous variables," Rev. Mod. Phys. **77**(2), 513–577 (2005).
9. R. Schnabel, N. Mavalvala, D. E. McClelland, and P. K. Lam, "Quantum metrology for gravitational wave astronomy," Nat. Commun. **1**(8), 121 (2010).
10. W. P. Bowen, R. Schnabel, N. Treps, H.-A. Bachor, and P. K. Lam, "Recovery of continuous wave squeezing at low frequencies," J. Opt. B Quantum Semiclassical Opt. **4**(6), 421–424 (2002).
11. R. Schnabel, H. Vahlbruch, A. Franzen, S. Chelkowski, N. Grosse, H.-A. Bachor, W. P. Bowen, P. K. Lam, and K. Danzmann, "Squeezed light at sideband frequencies below 100 kHz from a single OPA," Opt. Commun. **240**(1-3), 185–190 (2004).
12. J. Laurat, T. Coudreau, G. Keller, N. Treps, and C. Fabre, "Compact source of Einstein-Podolsky-Rosen entanglement and squeezing at very low noise frequencies," Phys. Rev. A **70**(4), 042315 (2004).
13. E. E. Mikhailov and I. Novikova, "Low-frequency vacuum squeezing via polarization self-rotation in Rb vapor," Opt. Lett. **33**(11), 1213–1215 (2008).
14. K. Goda, E. E. Mikhailov, O. Miyakawa, S. Saraf, S. Vass, A. Weinstein, and N. Mavalvala, "Generation of a stable low-frequency squeezed vacuum field with periodically poled KTiOPO4 at 1064 nm," Opt. Lett. **33**(2), 92–94 (2008).

#237089 Received 27 Mar 2015; revised 9 Jul 2015; accepted 28 Jul 2015; published 6 Aug 2015

15. H. Vahlbruch, A. Khalaidovski, N. Lastzka, C. Graf, K. Danzmann, and R. Schnabel, "The GEO600 squeezed light source," Class. Quantum Gravity **27**(8), 084027 (2010).
16. M. S. Stefszky, C. M. Mow-Lowry, S. S. Y. Chua, D. A. Shaddock, B. C. Buchler, H. Vahlbruch, A. Khalaidovski, R. Schnabel, P. K. Lam, and D. E. McClelland, "Balanced homodyne detection of optical quantum states at audio-band frequencies and below," Class. Quantum Gravity **29**(14), 145015 (2012).
17. The LIGO Scientific Collaboration, "A gravitational wave observatory operating beyond the quantum shot-noise limit," Nat. Phys. **7**, 962–965 (2011).
18. H. Vahlbruch, A. Khalaidovski, N. Lastzka, C. Gräf, K. Danzmann, and R. Schnabel, "The GEO 600 squeezed light source," Class. Quantum Gravity **27**(8), 084027 (2010).
19. K. Wodkiewicz and M. S. Zubairy, "Effect of laser fluctuations on squeezed states in a degenerate parametric amplifier," Phys. Rev. A **27**(4), 2003–2007 (1983).
20. D. D. Crouch and S. L. Braunstein, "Limitations to squeezing in a parametric amplifier due to pump quantum fluctuations," Phys. Rev. A **38**(9), 4696–4711 (1988).
21. J. Gea-Banacloche and M. S. Zubairy, "Influence of pump-phase fluctuations on the squeezing in a degenerate parametric oscillator," Phys. Rev. A **42**(3), 1742–1751 (1990).
22. P. K. Lam, T. C. Ralph, B. C. Buchler, D. E. McClelland, H.-A. Bachor, and J. Gao, "Optimization and transfer of vacuum squeezing from an optical parametric oscillator," J. Opt. B Quantum Semiclassical Opt. **1**(4), 469–474 (1999).
23. K. McKenzie, N. Grosse, W. P. Bowen, S. E. Whitcomb, M. B. Gray, D. E. McClelland, and P. K. Lam, "Squeezing in the audio gravitational-wave detection band," Phys. Rev. Lett. **93**(16), 161105 (2004).
24. K. Goda, K. McKenzie, E. Mikhailov, P. K. Lam, D. McClelland, and N. Mavalvala, "Photo thermal fluctuations as a fundamental limit to low-frequency squeezing in a degenerateoptical parametric oscillator," Phys. Rev. A **72**(4), 043819 (2005).
25. J. Gea-Banacloche and G. Leuchs, "Squeezed states for interferometric gravitational-wave detectors," J. Mod. Opt. **34**(6-7), 793–811 (1987).
26. B. Yurke, P. Grangier, and R. E. Slusher, "Squeezed-state enhanced two-frequency interferometry," J. Opt. Soc. Am. B **4**(10), 1677–1682 (1987).
27. Z. Zhai and J. Gao, "Low-frequency phase measurement with high-frequency squeezing," Opt. Express **20**(16), 18173–18179 (2012).
28. A. E. Dunlop, E. H. Huntington, C. C. Harb, and T. C. Ralph, "Generation of a frequency comb of squeezing in an optical parametric oscillator," Phys. Rev. A **73**(1), 013817 (2006).
29. R. J. Senior, G. N. Milford, J. Janousek, A. E. Dunlop, K. Wagner, H.-A. Bachor, T. C. Ralph, E. H. Huntington, and C. C. Harb, "Observation of a comb of optical squeezing over many gigahertz of bandwidth," Opt. Express **15**(9), 5310–5317 (2007).
30. R. Yang, J. Zhang, S. Zhai, K. Liu, J. Zhang, and J. Gao, "Generating multiplexed entanglement frequency comb in a nondegenerate optical parametric amplifier," J. Opt. Soc. Am. B **30**(2), 314–318 (2013).
31. M. A. Taylor, J. Janousek, V. Daria, J. Knittel, B. Hage, H.-A. Bachor, and W. P. Bowen, "Biological measurement beyond the quantum limit," Nat. Photonics **7**(3), 229–233 (2013).
32. M. Xiao, L. A. Wu, and H. J. Kimble, "Precision measurement beyond the shot-noise limit," Phys. Rev. Lett. **59**(3), 278–281 (1987).

1. Introduction

Squeezed and entanglement states are the key quantum resource, and have been applied to many important protocols in quantum information processing, such as gravitational-wave detection [1,2], quantum key distribution [3], quantum communication, quantum teleportation [4], quantum secret sharing [5], noiseless amplification [6], quantum dense coding [7], and quantum logic operation [8]. Some issues, such as gravitational-wave detection, magnetometer, atomic force microscopy, biological measurement, are appealing to obtain low-frequency squeezed state [9]. Low-frequency squeezing has attracted many interests in recent years. Squeezing below 300 kHz by optical parametric process was reported [10–12]. Squeezed vacuum light of 1 dB below shot-noise level(SNL) at 795 nm in Rb vapor via resonant polarization self-rotation was obtained from 30 kHz to 1.2 MHz in 2008 [13]. And lower frequency (Hz~kHz) squeezing were generated. The generation of a stable low-frequency squeezed vacuum field at 1064 nm using PPKTP in a subthreshold OPO has been demonstrated [14]. A squeezed quantum noise of up to 9 dB below the shot-noise level was observed in the detection band between 10 Hz and 10 kHz [15]. 10 dB of shot-noise suppression down to 10 Hz is directly observed [16]. Gravitational wave detectors are approaching their shot noise limit, which can be successfully overcome with squeezing at audio frequencies [17,18]. Optical parametric oscillators (OPO) are the common choice of systems to produce squeezed states. In fact, the level of low-frequency squeezing is usually limited by the introduction of noise from a variety of sources. The noise sources that limit the squeezing in these systems are pump noise [19–21], seed noise [22,23] and other excess

#237089 Received 27 Mar 2015; revised 9 Jul 2015; accepted 28 Jul 2015; published 6 Aug 2015

technical noise. Keisuke Goda *et al.* theoretically studied the effect of photothermal fluctuations on squeezed states of light through the photo-refractive effect and thermal expansion in a degenerate optical parametric oscillator (OPO) [24]. These frequency range represent a different regime experimentally to the majority of squeezed state production. It is more difficult to get low-frequency squeezing because of the potential limitation of noise sources.

An alternative way to conquer this difficulty is combining two-frequency laser with broadband squeezing at higher frequency. J. Gea-Banacloche and G. Leuchs theoretically showed that, in Michelson interferometers stabilized with phase modulation technique, broadband squeezing is needed [25]. Yurke et al proposed a two-frequency interferometer with a squeezed state to perform sub-shot-noise measurement of low-frequency signals [26]. A two-frequency intense laser and a squeezed light of high-frequency sidebands are applied in the interferometry instead of a one-frequency laser as usual [27].

In this paper, we propose a scheme for generation of low-frequency squeezing immune to laser technical noise from frequency comb, which can be used to enhance the squeezing degree directly for the same squeezing generator, and the signal-to-noise ratio (SNR) can be improved greatly for quantum measurement. This technique of low-frequency squeezing from frequency comb can be applied in some existing experiments. It can avoid the impact of those excess noises of low-frequency, and higher bandwidth photodetectors are not necessary anymore.

2. Low-frequency squeezing generated from optical frequency comb

Non-classical states of light are commonly generated via non-linear optical processes, such as parametric down conversion (PDC), in which a pump photon is converted into two photons of lower energy by a second order nonlinear interaction. The nonlinear optical parametric devices, such as degenerate optical parametric amplifier (DOPA) and non-degenerate optical parametric amplifier (NOPA), are the typical sources of squeezed and entangled light in the so-called continuous-variable regime. The optical cavity, which is used to increase the strength of the non-linear process, leads to spectral filtering of the down conversion output. The spectrum of down conversion fields are separated in frequency by the cavity free spectral range [FSR]. The phase matching bandwidth of the crystal in the optics cavity is much broader than FSR. Some unique properties such as squeezed and entangled frequency combs based on these quantum systems have been studied in recent years [28–30]. We consider two pairs of lower energy photons at least, one pair have same frequency (ω_L) and same polarization, the other pair have different frequency ($\omega_L \pm \mathrm{FSR}$) and same polarization, which can be simultaneously generated from an optical cavity with a crystal and the same pump ($2\omega_L$).

Figure 1 shows the scheme of low-frequency squeezing generated from NOPA, which provides two pairs of longitudinal modes. And a homodyne detection system with a two-frequency local beam is included. NOPA consists of a two-sided cavity and a nonlinear crystal.

#237089 Received 27 Mar 2015; revised 9 Jul 2015; accepted 28 Jul 2015; published 6 Aug 2015

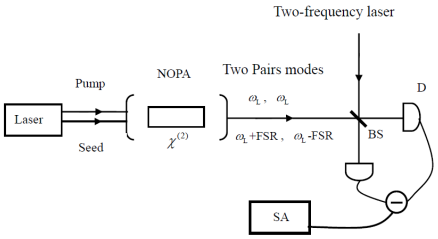

Fig. 1. The scheme of a low-frequency squeezing generated from squeezed frequency comb of NOPA. $\chi^{(2)}$: Nonlinear crystal, BS: Beam splitter, D: Photo-detector, SA: Spectrum analyzer.

We consider that the optical parametric process is in the triply resonating optical cavity with a nonlinear $\chi^{(2)}$ crystal.

The interaction Hamiltonian of optical parametric process in this NOPA is

$$H = i\hbar\chi^{(2)}(\hat{a}_0^{\dagger}\hat{a}_+\hat{a}_- - \hat{a}_0\hat{a}_+^{\dagger}\hat{a}_-^{\dagger}). \tag{1}$$

In the ideal case (with perfect phase matching), the equations of cavity mode after a single cavity round trip for the signal and idler modes can be expressed as

$$\hat{a}_+(t+\tau) = e^{i\Delta\tau}[-\chi\tau\hat{a}_-^{\dagger}(t) + (1-k\tau)\hat{a}_+(t) + \sqrt{2k}\tau\hat{b}_+^{in}(t) + \sqrt{2\gamma}\tau\hat{c}_+(t)], \tag{2}$$

$$\hat{a}_-(t+\tau) = e^{i\Delta\tau}[-\chi\tau\hat{a}_+^{\dagger}(t) + (1-k\tau)\hat{a}_-(t) + \sqrt{2k}\tau\hat{b}_-^{in}(t) + \sqrt{2\gamma}\tau\hat{c}_-(t)]. \tag{3}$$

Here, $\hat{a}_0$, $\hat{a}_+$ and $\hat{a}_-$ are the annihilation operators of intra-cavity pump mode, signal and idler modes, $\hat{b}_+^{in}$, $\hat{b}_-^{in}$ denote the annihilation operators of input fields. $\hat{c}_+$, $\hat{c}_-$ are the annihilation operators of vacuum, which correspond to the intra-cavity optical losses. $\chi^{(2)}$ is the effective nonlinear coupling parameter. It can be merged into pump field amplitude α_0 and considered as χ . The cavity transmission factor of two modes are assumed to be equal, and the same treatment for the extra-losses of two modes, $k_+ = k_- = k$ and $\gamma_+ = \gamma_- = \gamma$ .The detuning between the cavity mode and the cavity resonant frequency is Δ .

When the cavity is resonant with the cavity mode, $\Delta = 0$, We can expand the field operators in fluctuations around their respective mean values as $\hat{a}_i = \alpha_i + \delta\hat{a}_i$. After taking Fourier transforms, the following equations in the frequency domain can be obtained as

$$\delta\hat{a}_+(\omega)[e^{i\omega\tau} - (1-k\tau)] = -\chi\tau\delta\hat{a}_-^{\dagger}(\omega) + \sqrt{2k}\tau\delta\hat{b}_+^{in}(\omega) + \sqrt{2\gamma}\tau\delta\hat{c}_+(\omega), \tag{4}$$

$$\delta\hat{a}_-(\omega)[e^{i\omega\tau} - (1-k\tau)] = -\chi\tau\delta\hat{a}_+^{\dagger}(\omega) + \sqrt{2k}\tau\delta\hat{b}_-^{in}(\omega) + \sqrt{2\gamma}\tau\delta\hat{c}_-(\omega). \tag{5}$$

By the complex calculation for Eq. (4)and (5), the fluctuations of intra-cavity fields can be get as

$$\delta\hat{a}_+(\omega) = \frac{[\sqrt{2k}\tau\delta\hat{b}_+^{in}(\omega) + \sqrt{2\gamma}\tau\delta\hat{c}_+(\omega)][e^{i\omega\tau} - (1-k\tau)]}{[e^{i\omega\tau} - (1-k\tau)]^2 - \chi^2\tau^2} - \frac{\chi\tau^2[\sqrt{2k}\delta\hat{b}_-^{in\dagger}(\omega) + \sqrt{2\gamma}\delta\hat{c}_-^{\dagger}(\omega)]}{[e^{i\omega\tau} - (1-k\tau)]^2 - \chi^2\tau^2}, \tag{6}$$

$$\delta\hat{a}_-(\omega) = \frac{[\sqrt{2k}\tau\delta\hat{b}_-^{in}(\omega) + \sqrt{2\gamma}\tau\delta b\hat{c}_-(\omega)][e^{i\omega\tau} - (1-k\tau)]}{[e^{i\omega\tau} - (1-k\tau)]^2 - \chi^2\tau^2} - \frac{\chi\tau^2[\sqrt{2k}\delta\hat{b}_+^{in\dagger}(\omega) + \sqrt{2\gamma}\delta\hat{c}_+^{\dagger}(\omega)]}{[e^{i\omega\tau} - (1-k\tau)]^2 - \chi^2\tau^2}, \tag{7}$$

#237089 Received 27 Mar 2015; revised 9 Jul 2015; accepted 28 Jul 2015; published 6 Aug 2015

By using the boundary condition $\delta\hat{A}_{\pm}^{out}=\sqrt{2k}\delta\hat{a}_{\pm}-\delta\hat{b}_{\pm}^{in}$, we can get the amplitude and phase quadrature variances ($V_{+}^{x,y}$, $V_{-}^{x,y}$) of the two non-degenerate frequency longitudinal output modes:

$$\begin{aligned}V_{+}^{x,y}(\omega)=&\left|\frac{k^2+\chi^2-(\frac{1-e^{i\omega\tau}}{\tau})^2}{(k-\frac{1-e^{i\omega\tau}}{\tau})^2-\chi^2}\right|^2 V_{+in}^{x,y}+\left|\frac{2k\chi}{(k-\frac{1-e^{i\omega\tau}}{\tau})^2-\chi^2}\right|^2 V_{-in}^{x,y}\\&+\left|\frac{2\sqrt{k\gamma}(k-\frac{1-e^{i\omega\tau}}{\tau})}{(k-\frac{1-e^{i\omega\tau}}{\tau})^2-\chi^2}\right|^2 V_{+c}^{x,y}+\left|\frac{2\chi\sqrt{k\gamma}}{(k-\frac{1-e^{i\omega\tau}}{\tau})^2-\chi^2}\right|^2 V_{-c}^{x,y},\end{aligned}\tag{8}$$

$$\begin{aligned}V_{-}^{x,y}(\omega)=&\left|\frac{k^2+\chi^2-(\frac{1-e^{i\omega\tau}}{\tau})^2}{(k-\frac{1-e^{i\omega\tau}}{\tau})^2-\chi^2}\right|^2 V_{-in}^{x,y}+\left|\frac{2k\chi}{(k-\frac{1-e^{i\omega\tau}}{\tau})^2-\chi^2}\right|^2 V_{+in}^{x,y}\\&+\left|\frac{2\sqrt{k\gamma}(k-\frac{1-e^{i\omega\tau}}{\tau})}{(k-\frac{1-e^{i\omega\tau}}{\tau})^2-\chi^2}\right|^2 V_{-c}^{x,y}+\left|\frac{2\chi\sqrt{k\gamma}}{(k-\frac{1-e^{i\omega\tau}}{\tau})^2-\chi^2}\right|^2 V_{+c}^{x,y}.\end{aligned}\tag{9}$$

Where the definitions of the amplitude and phase quadrature fluctuations of the output and input beams are

$$\begin{aligned}&\delta\hat{X}_{\pm}(\omega)=\delta\hat{A}_{\pm}^{out}(\omega)+\delta\hat{A}_{\pm}^{out}(-\omega)^{\dagger},\delta\hat{Y}_{\pm}(\omega)=i[\delta\hat{A}_{\pm}^{out}(\omega)-\delta\hat{A}_{\pm}^{out}(-\omega)^{\dagger}]\\&\delta\hat{X}_{\pm in}(\omega)=\delta\hat{b}_{\pm}^{in}(\omega)+\delta\hat{b}_{\pm}^{in}(-\omega)^{\dagger},\delta\hat{Y}_{\pm in}(\omega)=i[\delta\hat{b}_{\pm}^{in}(\omega)-\delta\hat{b}_{\pm}^{in}(-\omega)^{\dagger}]\\&\delta\hat{X}_{\pm c}(\omega)=\delta\hat{c}_{\pm}^{in}(\omega)+\delta\hat{c}_{\pm}^{in}(-\omega)^{\dagger},\delta\hat{Y}_{\pm c}(\omega)=i[\delta\hat{c}_{\pm}^{in}(\omega)-\delta\hat{c}_{\pm}^{in}(-\omega)^{\dagger}]\end{aligned}\tag{10}$$

The amplitude and phase quadrature variances of input and output fields are given by the formulas:

$$\begin{aligned}&V_{\pm}^{x}(\omega)=\langle\left|\delta\hat{X}_{\pm}\right|^2\rangle,V_{\pm}^{y}(\omega)=\langle\left|\delta\hat{Y}_{\pm}\right|^2\rangle,V_{\pm in}^{x}(\omega)=\langle\left|\delta\hat{X}_{\pm in}\right|^2\rangle,\\&V_{\pm in}^{y}(\omega)=\langle\left|\delta\hat{Y}_{\pm in}\right|^2\rangle,V_{\pm c}^{x}(\omega)=\langle\left|\delta\hat{X}_{\pm c}\right|^2\rangle,V_{\pm c}^{y}(\omega)=\langle\left|\delta\hat{Y}_{\pm c}\right|^2\rangle\end{aligned}\tag{11}$$

Then we consider the correlation of amplitude and phase quadrature variances (the sum of amplitude quadrature and the difference of phase quadrature) for the two output longitudinal modes. We can get

#237089 Received 27 Mar 2015; revised 9 Jul 2015; accepted 28 Jul 2015; published 6 Aug 2015

$$V_{+,-}^{x}(\omega)=\left|\frac{(k-\chi)^2-(\frac{1-e^{i\omega\tau}}{\tau})^2}{(k-\frac{1-e^{i\omega\tau}}{\tau})^2-\chi^2}\right|^2 V_{+in}^{x}+\left|\frac{(k-\chi)^2-(\frac{1-e^{i\omega\tau}}{\tau})^2}{(k-\frac{1-e^{i\omega\tau}}{\tau})^2-\chi^2}\right|^2 V_{-in}^{x}$$
$$+\left|\frac{2\sqrt{k\gamma}(k-\frac{1-e^{i\omega\tau}}{\tau}-\chi)}{(k-\frac{1-e^{i\omega\tau}}{\tau})^2-\chi^2}\right|^2 V_{+c}^{x}+\left|\frac{2\sqrt{k\gamma}(k-\frac{1-e^{i\omega\tau}}{\tau}-\chi)}{(k-\frac{1-e^{i\omega\tau}}{\tau})^2-\chi^2}\right|^2 V_{-c}^{x}, \tag{12}$$

$$V_{+,-}^{y}(\omega)=\left|\frac{(k-\chi)^2-(\frac{1-e^{i\omega\tau}}{\tau})^2}{(k-\frac{1-e^{i\omega\tau}}{\tau})^2-\chi^2}\right|^2 V_{+in}^{y}+\left|\frac{(k-\chi)^2-(\frac{1-e^{i\omega\tau}}{\tau})^2}{(k-\frac{1-e^{i\omega\tau}}{\tau})^2-\chi^2}\right|^2 V_{-in}^{y}$$
$$+\left|\frac{2\sqrt{k\gamma}(k-\frac{1-e^{i\omega\tau}}{\tau}-\chi)}{(k-\frac{1-e^{i\omega\tau}}{\tau})^2-\chi^2}\right|^2 V_{+c}^{y}+\left|\frac{2\sqrt{k\gamma}(\chi-k+\frac{1-e^{i\omega\tau}}{\tau})}{(k-\frac{1-e^{i\omega\tau}}{\tau})^2-\chi^2}\right|^2 V_{-c}^{y}. \tag{13}$$

The FSR is assumed to be $800/2\pi$ MHz, and the optical circular frequency (radian per second) is used for the calculation convenience. The transmission coefficient of output coupler is 5%, and the intra-cavity optical loss is 0.4% for two longitudinal modes. The correlation variances of the sum of amplitude quadrature and the difference of phase quadrature for two non-degenerate frequency longitudinal modes (ω_L +FSR , ω_L -FSR) versus the side-band frequency are shown in Fig. 2. It demonstrates that the two output modes are entangled. On the other hand, the two output modes are actually the entangled upper and lower sidebands for the degenerate frequency squeezing comb. We assume that the nonlinear coupling of the non-degenerate optical parametric process (ω_L +FSR , ω_L -FSR) is the same with that of the degenerate optical parametric process (ω_L , ω_L).

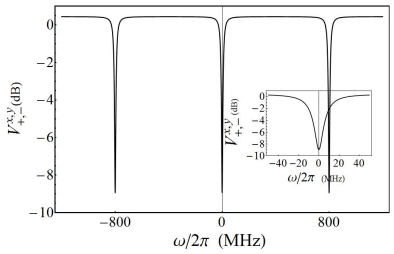

Fig. 2. The squeezed comb noise spectra *vs* the side-band frequency, Inset shows the detail of a comb tooth.

For most experiments, squeezing can be extended to tens of megahertz among high-frequency sidebands. In order to obtain the low-frequency squeezing, the experimental scheme utilizing the high-frequency sidebands of the squeezed light and a two-frequency local beam was proposed [27]. Instead of using one-frequency local beam at frequency ω_L in the balance homodyne detection system, a local beam with two carrier frequencies $\omega_L \pm \omega_i$, interfere with the entangled upper and lower sidebands of the comb for the generation of low-frequency squeezing. ω_L is the center frequency of the light, $2\omega_i$ is the frequency interval of the two-frequency local beam. $i=1,2$, denotes two kinds of two-frequency local beam.

#237089 Received 27 Mar 2015; revised 9 Jul 2015; accepted 28 Jul 2015; published 6 Aug 2015

The relaxation oscillation and other excess technical noise sources, which are commonly existing, have typically confined squeezing to MHz range, and leads to dramatic degradation of squeezing at low frequency [16,18]. Here, the amplitude quadrature is quantum noise limited and the phase quadrature noise is approximated as "1/ f" noise. Thus we set $V_{+in}^{x}=1$, $V_{-in}^{y}=1+\left|1000/\omega\right|$, and the technical noise is larger than the quantum noise limit inevitably for the low-frequency range [28]. All the factors, such as spontaneous emission noise, other technical noise consistent with existing laser, optical technologies and typical laboratory environments, are responsible for the low-frequency squeezing degradation. The phase quadrature noise spectra of output mode versus the side-band frequency are given in Fig. 3. As a result, the extra noise can reduce the squeezing level in the range of low frequency. And the squeezing vanishes near the zero frequency.

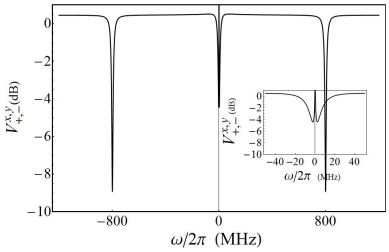

Fig. 3. Phase quadrature noise spectra of output versus side-band frequency. Inset shows the detail of the squeezing level of the zero-order tooth.

Now we have investigated the case of resonant. However, each tooth in the comb will carry the copies of noise from acoustic vibrations, thermal expansion and others. Such noise has degrading effects on the production of squeezing via optical path length fluctuations, which potentially causing a detuning of the optical cavity. We can lock the cavity in experiment to keep resonant. The small detuning has been considered in the model. Then the correlation noise of two output modes can be given by

$$
\begin{aligned}
V_{+,-}^{x}(\omega)=&\left|\frac{[(k-\frac{1-e^{i(\omega+\triangle)\tau}}{\tau})(k+\frac{1-e^{i(\omega-\triangle)\tau}}{\tau})+\chi^{2}-2k\chi}{(k-\frac{1-e^{i(\omega+\triangle)\tau}}{\tau})(k-\frac{1-e^{i(\omega-\triangle)\tau}}{\tau})-\chi^{2}}\right|^{2}V_{+in}^{x}\\
&+\left|\frac{[(k-\frac{1-e^{i(\omega+\triangle)\tau}}{\tau})(k+\frac{1-e^{i(\omega-\triangle)\tau}}{\tau})+\chi^{2}-2k\chi}{(k-\frac{1-e^{i(\omega+\triangle)\tau}}{\tau})(k-\frac{1-e^{i(\omega-\triangle)\tau}}{\tau})-\chi^{2}}\right|^{2}V_{-in}^{x}\\
&+\left|\frac{2\sqrt{k\gamma}(k-\frac{1-e^{i(\omega+\triangle)\tau}}{\tau}-\chi)}{(k-\frac{1-e^{i(\omega+\triangle)\tau}}{\tau})(k-\frac{1-e^{i(\omega-\triangle)\tau}}{\tau})-\chi^{2}}\right|^{2}V_{+c}^{x}\\
&+\left|\frac{2\sqrt{k\gamma}(k-\frac{1-e^{i(\omega+\triangle)\tau}}{\tau}-\chi)}{(k-\frac{1-e^{i(\omega+\triangle)\tau}}{\tau})(k-\frac{1-e^{i(\omega-\triangle)\tau}}{\tau})-\chi^{2}}\right|^{2}V_{-c}^{x}
\end{aligned}
\qquad (14)
$$

#237089 Received 27 Mar 2015; revised 9 Jul 2015; accepted 28 Jul 2015; published 6 Aug 2015

$$
\begin{aligned}
V_{+,-}^{y}(\omega)=&\left|\frac{[(k-\frac{1-e^{i(\omega+\Delta)\tau}}{\tau})(k+\frac{1-e^{i(\omega-\Delta)\tau}}{\tau})+\chi^2-2k\chi}{(k-\frac{1-e^{i(\omega+\Delta)\tau}}{\tau})(k-\frac{1-e^{i(\omega-\Delta)\tau}}{\tau})-\chi^2}\right|^2 V_{+in}^{y}\\
&+\left|\frac{[(k-\frac{1-e^{i(\omega+\Delta)\tau}}{\tau})(k+\frac{1-e^{i(\omega-\Delta)\tau}}{\tau})+\chi^2-2k\chi}{(k-\frac{1-e^{i(\omega+\Delta)\tau}}{\tau})(k-\frac{1-e^{i(\omega-\Delta)\tau}}{\tau})-\chi^2}\right|^2 V_{-in}^{y}\\
&+\left|\frac{2\sqrt{k\gamma}(k-\frac{1-e^{i(\omega+\Delta)\tau}}{\tau}-\chi)}{(k-\frac{1-e^{i(\omega+\Delta)\tau}}{\tau})(k-\frac{1-e^{i(\omega-\Delta)\tau}}{\tau})-\chi^2}\right|^2 V_{+c}^{y}\\
&+\left|\frac{2\sqrt{k\gamma}(\chi+\frac{1-e^{i(\omega+\Delta)\tau}}{\tau}-k)}{(k-\frac{1-e^{i(\omega+\Delta)\tau}}{\tau})(k-\frac{1-e^{i(\omega-\Delta)\tau}}{\tau})-\chi^2}\right|^2 V_{-c}^{y}
\end{aligned}
\tag{15}
$$

When $\Delta=\frac{0.3}{2\pi}$MHz , the noise spectrum in Figs. 4(a) and 4(b) have been given correspondingly using dot line compared with solid line of no detuning. The squeezing level is reduced from −9dB to −8.5dB for the first order tooth and from −4.5dB to −4.2dB for the zero-order tooth.

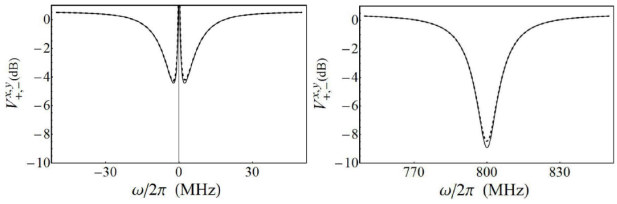

Fig. 4. Noise spectra with $\Delta=\frac{0.3}{2\pi}$MHz (dot line), $\Delta=0$ (solid line). (a) Squeezing of the zero-order tooth. (b) Squeezing of the first order tooth

3. Immunity to Laser technical noise for low-frequency squeezing

In this scheme, the two pairs of output longitudinal modes, correspond to the two-frequency local beam $\omega_L\pm\omega_1,\omega_1=\frac{2}{2\pi}$MHz or $\omega_L\pm\omega_2,\omega_2=\frac{800}{2\pi}$MHz . Here we choose the $\omega_L\pm\omega_2,\omega_2=\frac{800}{2\pi}$MHz local beam and the output of non-degenerate frequency longitudinal modes, and get a stronger low-frequency squeezing, which is not affected by the low frequency excess noise, and not restricted by the cavity bandwidth of NOPA, as can be seen in Fig. 5.

A low-frequency squeezing immune to laser technical noise can be obtained by the two-frequency local beam $\omega_L\pm\omega_2,\omega_2=\frac{800}{2\pi}$MHz . The noise spectrum versus low frequency is

#237089 Received 27 Mar 2015; revised 9 Jul 2015; accepted 28 Jul 2015; published 6 Aug 2015

given in Fig. 6. We can draw the conclusion that the low-frequency squeezing of −9dB is obtained with two-frequency laser of $\omega_L \pm \frac{800}{2\pi}$MHz .

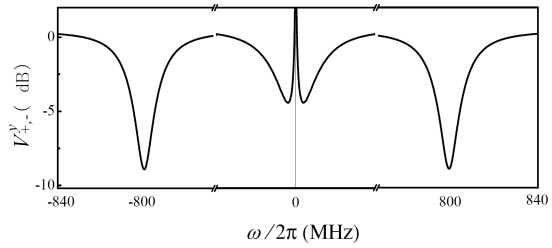

Fig. 5. Low-frequency squeezing by two-frequency local beam $\omega_L \pm \omega_1$, $\omega_1 = \frac{2}{2\pi}$MHz and $\omega_L \pm \omega_2, \omega_2 = \frac{800}{2\pi}$MHz , respectively.

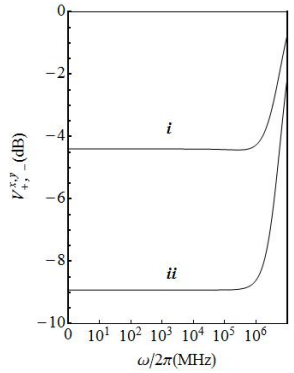

Fig. 6. The noise spectra in low frequency domain. Two curves correspond to two kinds of two-frequency laser: curve *i*, $\omega_L \pm \frac{2}{2\pi}$MHz ; curve *ii*, $\omega_L \pm \frac{800}{2\pi}$MHz .

Considering of two other schemes of squeezing measurement, continuous wave (CW) operation with one squeezing beam, modulated local beam or modulated squeezer [31], it's necessary to compare them using the same parameters for the laser noise and the squeezing apparatus. Squeezing level of −5dB at 2MHz can be measured by traditional CW operation with one squeezed beam, but the low-frequency squeezing (Hz~kHz) cannot be obtained because of extra noise. Low-frequency squeezing of −5dB can be extracted if the frequency of modulated LO equals to $\frac{2}{2\pi}$MHz for the zero-order tooth.

4. Phase measurement with low-frequency squeezing

The SNR can be enhanced with low-frequency squeezing for phase measurement with an interferometer.

A squeezing-enhanced Mach-Zehnder interferometer was shown in [32]. By means of a two-frequency laser interferometer and higher-frequen cy sidebands of the squeezed state, the SNR of lower-frequency phase measurement can be enhanced [27]. The SNR can be expressed as [27]

$$SNR = \frac{2NT\theta_{\Omega}^2}{V_b^{\varphi+\pi/2}(\Omega + w_i) + V_b^{\varphi+\pi/2}(\Omega - w_i)}. \quad (16)$$

#237089 Received 27 Mar 2015; revised 9 Jul 2015; accepted 28 Jul 2015; published 6 Aug 2015

Here, the average photon number in unit measurement time is $N = P/\hbar\omega_{\mathrm{L}}$, where P is the optical power of the two-frequency laser. Photocurrent duration is T, which is the reciprocal of measurement resolution bandwidth (RBW). θ_{Ω} is the signal amplitude at frequency Ω. $V_b^{\varphi+\pi/2}(\Omega \pm w_i)$ is the quadrature variance of the squeezed state at frequency $\Omega \pm w_i$.

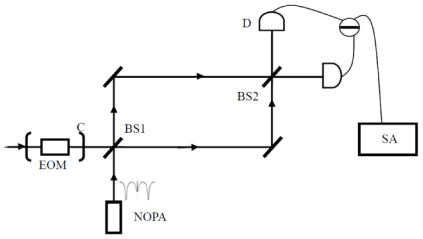

Fig. 7. Application of low-frequency squeezing for phase measurement in Mach-Zehnder interferometer. EOM: Electro optic modulator, C: Cavity, BS1, BS2: Beam splitter, D: Photo-detector, SA: Spectrum analyzer.

A scheme of the SNR enhancement of quantum measurement in Mach-Zehnder interferometer is given in Fig. 7. The relative phase at the first 50% beam splitter is φ, and the relative phase at the second 50% beam splitter is $\pi/2$. An electro optic modulator (EOM) is inside the cavity, which can provide the two-frequency laser. The power of two-frequency laser is 1mw, the wavelength is 1064nm, the RBW is 100KHz. Ω is very small for the low-frequency signal, therefore the variance of $V_b^{\varphi+\pi/2}(\Omega \pm w_i)$ can be considered as the same with $V_b^{\varphi+\pi/2}(\omega_i)$. Here, the SNR of 3dB signal is assumed to be 1, and the calculated minimum phase is $\theta_{\Omega} = 0.38*10^{-5}$. SNR versus frequency is shown in Fig. 8. The two curves correspond to two kinds of two-frequency laser: curve *i*, $\omega_{\mathrm{L}} \pm \frac{2}{2\pi}$MHz ; curve *ii*, $\omega_{\mathrm{L}} \pm \frac{800}{2\pi}$MHz . It is found that this kind of low-frequency squeezing can enhance the level of SNR for phase measurement indeed.

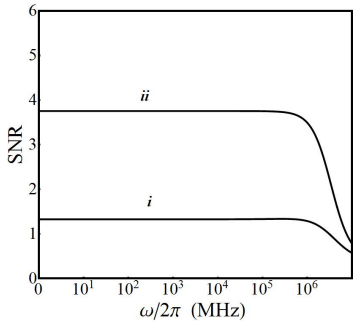

Fig. 8. SNR *vs* frequency for low-frequency phase measurement in Mach-Zehnder interferometer with two kinds of two-frequency laser, curve *i*, $\omega_{\mathrm{L}} \pm \frac{2}{2\pi}$MHz ; curve *ii*, $\omega_{\mathrm{L}} \pm \frac{800}{2\pi}$MHz .

#237089 Received 27 Mar 2015; revised 9 Jul 2015; accepted 28 Jul 2015; published 6 Aug 2015

5. Conclusion

In conclusion, we have proposed a scheme of low-frequency squeezing immune to laser technical noise from squeezed comb with a two-frequency laser, and investigated the SNR enhancement of phase measurement in Mach-Zehnder interferometer with the low-frequency squeezing. We hope that this low-frequency squeezing may be helpful for quantum measurement. Limitations of the present scheme for the gravitational-wave detection exist indeed because that the FSR and mode structure of displacement enhanced cavity need to be the same as that of the squeezer exactly. But this scheme is promising in many metrology and sensor applications. If we can separate the two output longitudinal modes spatially by using dispersion element, the low-frequency entanglement will be generated from this NOPA, even many pairs of low-frequency EPR beams can be obtained from the entangled comb. It will be a valuable resource for quantum information.

Acknowledgments

This work was supported by the Program National Natural Science Foundation of China (Grant Nos.61108003, 11274210, 11174189), the Natural Science Foundation of Shanxi (Grant Nos.2013021005-2) and the National Key Basic Research Program of China (973 Program) (Grant Nos.2010CB923102).

#237089 Received 27 Mar 2015; revised 9 Jul 2015; accepted 28 Jul 2015; published 6 Aug 2015